Role of ERK2 dimerization in synaptic plasticity and memory

Ojea Ramos, Santiago[1]; Medina, Candela[3]; Krawczyk, María del Carmen[3*]; Millan, Julieta[3*]; Acutain, María Florencia[4*]; Romano, Arturo Gabriel[1,2]; Baez, María Verónica[4]; Urbano, Francisco José[1,2]; Boccia, Mariano Martín[3]; Feld, Mariana[1#]

* Equal contribution

[1] Instituto de Fisiología, Biología Molecular y Neurociencias (IFIBYNE), Universidad de Buenos Aires (UBA) – Consejo Nacional de Investigaciones Científicas y Técnicas (CONICET).

[2] Departamento de Fisiología, Biología Molecular y Celular "Prof. Héctor Maldonado", Facultad de Ciencias Exactas y Naturales, UBA.

[3] Laboratorio de Neurofarmacología de Procesos de Memoria, Cátedra de Farmacología, Facultad de Farmacia y Bioquímica – UBA.

[4] Instituto de Biología Celular y Neurociencias "Prof. Dr. E. de Robertis" (IBCN), CONICET - UBA.

[#], corresponding author: mfeld@fbmc.fcen.uba.ar

ABSTRACT

Extensive research has focused on extracellular-signal regulated kinase 1/2 (ERK) phosphorylation in different memory and plasticity models. However, the precise mechanism by which ERK activity leads to memory stabilization and restabilization remains largely elusive, and little is known about the role of ERK 1/2 dimerization in those processes. ERK dimerization is critical for the binding and activation of extranuclear targets, some of which have been strongly associated with these processes. Here we report for the first time that ERK2 dimerization occurs in the context of the rodent nervous system and plays a critical role in plasticity and memory processes. ERK2 dimerization was blocked by DEL-22379 (DEL), a recently developed specific ERK dimerization inhibitor in mice hippocampus in vivo. Moreover, DEL impaired high frequency stimulation-induced long-term potentiation in acute hippocampal slices. However, inhibitory avoidance (IA) memory reactivation induced a significant decrease of ERK2 dimerization in hippocampi from weak IA-trained mice. Noteworthily, intrahippocampal infusion of the inhibitor after memory reactivation had a surprising bidirectional effect: while it blocked reconsolidation of a strong IA memory, the opposite effect was observed on reconsolidation of a weak IA memory, resulting in its enhancement.
Although more research is needed, these initial findings suggest a relevant role of ERK dimerization in plasticity and memory.

INTRODUCTION

Molecular mechanisms involved in learning and memory have been extensively assessed in the last decades using a wide variety of paradigms and techniques. Long-term plasticity is considered the cellular correlate of memory formation [1,2]. In line with this proposal, certain signaling pathways have been associated with both plasticity and memory processes. Particularly, extracellular signal-regulated kinase 1/2 (ERK1/2) phosphorylation has been shown to subserve both of them [3–8, and others]. Pharmacological assays demonstrated that ERK1/2 inhibition impairs memory as well as plasticity[reviewed in 9]. Mitogen-activated protein kinase (MAPK) family, including ERK1/2 cascade, is a large group of Ser/Thr protein kinases that were initially associated with development, mitogenesis, and stress response[10]. ERK activation is achieved through phosphorylation of residues Thr185 and Tyr187 (human numbering) in a common TEY motif (pERK hereafter) which then translates into conformational changes leading to substrate binding and phosphorylation. Although initial results suggested that activation of the protein by phosphorylation led to dimerization and subsequent nuclear translocation, it was later disclosed that in fact dimerization guides extra-nuclear function[11], and contributes to binding and activation of cytosolic targets aided by scaffolding proteins[12]. Consistently, ERK dimerization inhibition blocked cytoplasmic but not nuclear signaling[13]. Moreover, the multiplicity of ERK1/2 cytosolic targets described in past years[14–19] supports the idea that extranuclear localization of the kinase is relevant for a wide variety of processes apart from gene expression regulation. Less than a decade ago, Herrero and colleagues[13] described a novel compound that inhibits ERK dimerization (DEL-22379, DEL hereafter) and blocked the growth of hyperactive Ras-ERK1/2 signaling tumor cells, without decreasing its effectiveness by resistance mechanisms described for phosphorylation inhibitors. Thus, preventing ERK dimerization attenuated cellular proliferation, transformation and tumor development. Oncologic research contributed to the understanding of ERK´s role in general cell function. However, ERK1/2 neuronal activation shall certainly show specific hallmarks depending on subcellular localization and kinetics in the context of processes such as synaptic plasticity, learning and memory.

The role of ERK activation in synaptic plasticity and memory processes has been extensively studied although scarce information on specific function in different subcellular compartments is available. pERK expression was increased at pre- and postsynaptic sites from pyramidal neurons of the visual cortex after in vivo visual stimulation in dark-reared rats and its temporal profile was similar to ERK activation in neuronal cell bodies[20]. High-frequency stimulation selectively induced ERK activation, regulating translation at specific subcellular compartments at active synapses in the medial perforant pathway[21]. Cytoplasmic localization of ERK depends on expression levels of several anchor proteins such as MEK[22], MAP kinase phosphatase 3 (MKP3)[23] or scaffold proteins such as the actin cytoskeleton-interacting protein IQGAP1 (IQ Motif Containing GTPase Activating Protein 1), which mediates ERK binding to actin filaments[24]. Moreover, NR2A-induced ERK activation was shown to have a role in the regulation of dendritic spine density in key brain areas involved in cognition[25]. It also accounts for neurodegenerative pathologies, depending on the stage of development of the organism, the type of cellular element in which the pathway is activated and the anatomical neuronal structure[26].

Stability of consolidated memories can be challenged by reactivation, opening a new period of sensitivity named ‘‘reconsolidation” and triggering molecular mechanisms involved in re-

stabilization[27–29]. Previous work from our group revealed that cytosolic ERK activation is important for the consolidation and reconsolidation of memories in invertebrates and vertebrates, respectively. In the Context-Signal Memory of the crab *Neohelice granulata* (formerly called *Chasmagnathus granulatus*), extra-nuclear ERK became active specifically one hour after an associative learning took place[30]. Reactivation of an inhibitory avoidance memory in CF-1 mice governed three different processes according to ERK cytosolic kinetics[31–33]. Moreover, ERK overactivation including nuclear ectopic phosphorylation accounted for memory impairment as partial inhibition of the pathway reverted the deficit in a mouse model of Alzheimer's disease[34]. These results evidence a disregarded phenomenon which deserves further attention.

While ERK1/2 phosphorylation has been extensively studied regarding memory and plasticity, there is no report on the role of dimerization in these processes. We hypothesized that cytosolic action of ERK1/2 regulated by dimerization constitutes a regulatory milestone for long-term memory (LTM) consolidation and reconsolidation. Here we show for the first time that ERK2 dimerization can be pharmacologically inhibited in mice hippocampi without affecting phosphorylation. This inhibition blocked CA1 hippocampal LTP and affected memory reconsolidation depending on the strength of inhibitory avoidance (IA) task (it impaired a strong memory while improving a weak one). This is the first report on ERK dimerization role *in vivo* in the nervous system and on memory processes. These initial findings support a key role of ERK dimerization in plasticity and memory.

Materials and Methods

Animals.

Different cohorts of CF-1 male mice aged either 5 (weight range: 32.5 - 37.2 g, housed in groups of 3-5 individuals in 18.41 x 29.21 x 12.7 cm amber polysulfone cages) or 8-10 weeks old (weight range: 25-30 g, housed in groups of 10-12 individuals in stainless-steel 50 x 30 x 15 cm^3 cages) were used either for electrophysiological experiments or behavioral and pharmacological testing, respectively. The mice had *ad libitum* access to dry food and tap water and were maintained under a 12h light/dark cycle (lights on at 6:00 AM) at a temperature of 21-23ºC. Mice were bred in-house at the Facultad de Farmacia y Bioquímica, Universidad de Buenos Aires. Experiments were conducted during the light cycle. All procedures related to care and treatments of mice were approved by the local institutional animal care and use committees (CICUAL - CUDAP # 0044975-2016, Facultad de Farmacia y Bioquímica; CICUAL 154b, Facultad de Ciencias Exactas y Naturales, Universidad de Buenos Aires, Argentina), and in compliance with the standard European Union and United States National Institutes of Health ethical guidelines for Care and Use of Laboratory Animals. All efforts were made to minimize any possible distress or suffering experienced by mice, as well as to reduce the number of animals required to generate reliable scientific data.

Drugs.

DEL-22379 (DEL), an ERK dimerization inhibitor[13], was purchased from MedChemExpress (Cat. No.: HY-18932) and dissolved in dimethyl sulfoxide (DMSO) as a vehicle (VEH). For behavioral experiments and hippocampal ERK2 dimerization assays, 0.5 µl of drug or VEH solution were injected per hemi-hippocampus (final concentration of DEL used: 500 nM). Epidermal growth-factor (EGF) was purchased from Thermo Fisher (Cat. No.: PHG0314) and diluted in sterile PBS to a final concentration of 100 µM (stock solution).

Hippocampal slices and whole-cell patch-clamp recordings.

Electrophysiological recordings in slices were performed as described elsewhere[35]. Briefly, mice were deeply anesthetized with a mix of ketamine (160 mg/kg) and xylazine (8 mg/kg) before decapitation. Coronal brain slices including dorsal hippocampus (300-400 µm) were obtained by gluing the brain onto a vibratome stage (PELCO, EasiSlicer, Ted Pella Inc., CA, USA), submerged in a chamber containing chilled low-sodium/high-sucrose solution (250 mM sucrose, 2.5 mM KCl, 3 mM $MgSO_4$, 0.1 mM $CaCl_2$, 1.25 mM NaH_2PO_4, 0.4 mM ascorbic acid, 3 mM myo-inositol, 2 mM pyruvic acid, 25 mM D-glucose, and 25 mM $NaHCO_3$). Sequential slices obtained and Schaffer collaterals were transected near CA3 before being transferred to an incubation chamber and kept at 35 °C for 30 min containing low Ca^{2+} /high Mg^{2+} normal artificial cerebrospinal fluid (ACSF; 125 mM NaCl, 2.5 mM KCl, 3 mM $MgSO_4$, 0.1 mM $CaCl_2$, 1.25 mM NaH_2PO_4, 0.4 mM ascorbic acid, 3 mM myo-inositol, 2 mM pyruvic acid, 25 mM d-glucose, and 25 mM $NaHCO_3$ and aerated with 95% O_2/5% CO_2, pH 7.4). Slices were then transferred to the recording chamber and perfused continuously with ACSF including bicuculline (20 µM; a GABA-A antagonist).
Recording electrodes were made with borosilicate glass (2–3 MΩ) filled with ACSF + bicuculline solution and placed in the *stratum radiatum* area of the CA1 region of the hippocampus. The field excitatory postsynaptic potential (fEPSP) were recorded as a measure of excitatory synaptic transmission in the CA1 region. The stimulating electrode was placed at the Schaffer Collateral fibers and fEPSPs were evoked by test stimuli (0.033 Hz, 0.05-0.2 ms duration) every 30 sec. LTP was induced by applying high frequency stimulation (HFS; 5 trains, 100 Hz, 10 pulses) after a recorded baseline period of 10 min. Recordings were maintained for 30 min after LTP induction. The magnitude of LTP was calculated as a percentage of the averaged fEPSP slope value after HFS achieved the baseline fEPSP slope value. Changes in LTP were compared in hippocampal slices incubated with either DEL (30 min., 1,33 uM) or VEH. Signals were recorded using a MultiClamp 700 amplifier commanded by pCLAMP 10.0 software (Molecular Devices, CA, USA). Data was filtered at 5 kHz, digitized, and stored for off-line analysis.

Intra-hippocampal injections.

Hippocampal injections were performed under isoflurane anesthesia (induction: 3.5 %, maintenance: 1 %) using a stereotaxic apparatus (Stoelting) at the indicated time points. Surgery lasted for no more than 15 min. A small incision was made in the scalp and two holes were drilled in the skull at the following coordinates: AP: -1.90 mm from bregma, DV: -1.2 mm from the skull surface and +/-1.5 mm left and right from the midsagittal suture[36] to bilaterally infuse the drugs. A 30 gauge stainless steel needle attached to a 5 µl Hamilton syringe through PE-10 tubing was used for the infusion. The drug infusion lasted 60 sec and the needle was left in place for another 30 sec to avoid reflux. Total volume administration was 0.5 µl (either drug or VEH) per hemi-hippocampi. At the end of the procedure, the incision was sutured and thoroughly disinfected. After the last testing session, animals were euthanized by cervical dislocation and brains were dissected, fixed by immersion in 4 % PFA overnight, and sectioned to verify the correct injection site placement. In all cases administration placement was confirmed in the target area.

Inhibitory Avoidance task.

IA behavior was studied using a one-trial step-through protocol, which takes advantage of mice's natural preference for dark and confined spaces [37,38]. The apparatus consists of a dark closed compartment (20 x 20 x 15 cm) with a stainless-steel grid floor and a small illuminated open platform (5 x 5 cm) attached to its entrance. During the training phase (TR), each mouse was placed on the illuminated platform and received a foot shock upon entry into the dark compartment. Two different shock intensities were used: a 0.3 mA - 3 sec shock for weak

inhibitory avoidance induction (wIA) and a 0.4 mA - 3 sec shock for strong inhibitory avoidance (sIA) memory formation[39]. Mice underwent two retention tests after TR. The first retention test (T1), 48 h after TR, followed by a second retention test (T2) 24 h after T1. No shock was delivered during either test session. T1 also induced memory reactivation (RE), and this process was controlled by means of a non-reactivated (NR) group. The retention tests were finished either when the mouse stepped into the dark compartment or failed to enter within 300 sec after the beginning of the test. After the retention test, mice were returned to their homecage. Step through latencies were manually registered by the experimenter using a chronometer.

Sample preparation and ERK analysis.

Neuronal cultures. Primary neuronal cultures were obtained as described before[40] according to Kaech and Banker´s method[41]. Briefly, Wistar embryos were obtained on day 17 (E17), both hippocampi were dissected from pups and digested with trypsin (Sigma, Sigma–Aldrich Co., St. Louis, MO, United States). Cells were plated onto poly-L-lysine (Sigma)–coated wells and incubated in neurobasal media (NB; Invitrogen, Life Technologies Corporation, Carlsbad, CA, United States) supplemented with B27 (Invitrogen) and Glutamax (Invitrogen). Cultures were maintained in complete NB (NB + B27 + Glutamax) at 37°C and with 5% CO_2. Culture media were replaced by 1/3 every 2 days.
For the induction of ERK activation by EGF, 1 µl of the stock solution was diluted in 1 mL of culture medium and incubated in the culture for 5 minutes. On the other hand, chemical LTP (cLTP) induction was achieved by a glycine stimulation protocol previously described[42] with some modifications. Neuronal cultures were incubated with conditioned media containing 200 mM glycine for 3 min. Glycine solution was then removed and neurons were incubated in their media for 2 or 13 min to complete 5 or 15 min of incubation. Control groups were incubated with conditioned media for 3 min without Glycine stimulation.
After treatment, neuronal cultures were cooled and homogenized by scraping cells in ice-cold lysis buffer (20 mM Hepes, pH 7.5, 10 mM ethylene glycol tetraacetic acid, 40 mM glycerol 2-phosphate, 1 % (w/v) IGEPAL, 2.5 mM $MgCl_2$, 2 mM orthovanadate, 1 mM dithiothreitol, 0.5 mM PMSF, 50 mM Sodium Fluoride, 1 µg/ml Pepstatin A, 10 µg/mL Leupeptin, 10 µg/mL Aprotinin). Samples were centrifuged at 13000 x g for 10 min at 4 ºC, and the supernatants were collected and conserved at -20 ºC.

Hippocampal tissue. For the induction of hippocampal ERK activation by EGF, two injections were performed in each hemi-hippocampus: 0.5 µl of the stock EGF solution or vehicle (PBS, CT); ii) 0.5 µl of 400 nM DEL or vehicle (DMSO, VEH). At the specified time points mice were quickly euthanized by cervical dislocation, decapitated and the hippocampi were dissected. Tissue was then homogenized using a Dounce tight homogenizer and 250 µL of ice-cold lysis buffer (20 mM Hepes, pH 7.5, 10 mM ethylene glycol tetraacetic acid (EGTA), 40 mM glycerol 2-phosphate, 1 % (w/v) IGEPAL, 2.5 mM $MgCl_2$, 2 mM orthovanadate, 1 mM dithiothreitol, 0.5 mM PMSF, 50 mM Sodium Fluoride, 1 µg/ml Pepstatin A, 10 µg/mL Leupeptin, 10 µg/mL Aprotinin) by performing 8 strokes with a tight glass pestle. Samples were centrifuged at 13000 x g for 10 min at 4 ºC, and the supernatants were collected and conserved at -20 ºC.

Native gel electrophoresis. Native polyacrylamide gel electrophoresis (PAGE) for ERK dimers detection was carried out as described previously[43]. Briefly, protein levels in lysates were quantified by BCA Assay (Bio-Rad, USA) and 60 µg of protein were loaded into a 8 % bis-acrylamide gel and run for 150 min at 70 V. Then samples were transferred to a nitrocellulose membrane (General Electric, USA) overnight at 125 mA and 4 ºC.

SDS-PAGE. ERK phosphorylation levels were assessed by means of denaturing gel electrophoresis as described elsewhere[31]. Briefly, 20 µg of protein were loaded in a 12.5 % bis-acrylamide gel and run for 90 min at 100 V. The samples were then transferred to a PVDF membrane (Thermo Scientific, USA) overnight at 300 mA and 4 ºC and stored in TBS until probed with antibodies.

Antibodies used and detection. Initially, all membranes were blocked in 4% non-fat dry milk in TBS - 0.05 % Tween20. A full list of antibodies used, and dilutions can be found in Table 1. Primary antibodies were incubated overnight at 4 ºC and secondary antibodies were incubated for 1 h in TTBS at room temperature. ERK dimers were detected on nitrocellulose membranes by luminol chemiluminescence kit (Bio Rad ECL, USA) using X-Ray film (Agfa ORTHO CP-GU, cat. PTNAGCPGUM2, Voxel, Argentina). SDS-PAGE blots were developed using the same chemiluminescence kit in a GE Amersham Imager.

Table 1.

Target	Supplier	Carrier solution	Dilution
ERK2	Santa Cruz (SC-1647)	4 % milk in TBS - 0.5 % (v/v) Tween	1:1000
pERK1/2	Cell Signaling (9101)	4 % milk in TBS - 1 % (v/v) Tween	1:2000
ERK1/2	Cell Signaling (9102)		1:2000
Anti Rabbit	Santa Cruz (SC-2357)		1:10000
Anti Mouse	Cell Signaling (7076)		1:15000

Data analysis.

Data analyses were conducted using R (version 4.2.2,83). Generalized linear models (GLMs) were employed using the glmmTMB package (version 1.1.6). For behavioral data (latency to step-through), drug (VEH or DEL) and condition (RE or NR) were used as fixed factors. The model was fitted with a Gamma distribution and log link function. For western blot data, the model was fitted using a Gaussian distribution and identity link function. In the LTP experiment, Time was added as a fixed factor in order to account for repeated measures. The goodness-of-fit for each model was analyzed using the DHARMa package (version 0.4.6). Visual inspection of residual plots did not reveal any concerning deviations from normality or homoscedasticity. Anova of the models is reported and, when applicable, post-hoc comparisons were performed using the emmeans package (version 1.8.5). All reported p-values were adjusted for multiple comparisons with the Šidak correction method. Two-tailed Pearson coefficients were calculated to determine the correlation between phosphorylation and dimerization at each time point.

Results

ERK dimerization in rodent nervous system and plasticity

The latency to enter the dark compartment in the inhibitory avoidance (IA) task depends on the intensity of the stimulus applied to the animal during training. Previous results from our group using the IA task in CF-1 mice showed that reactivation of a consolidated memory (i.e.

by memory retrieval) induced different levels of cytosolic phosphorylated ERK2 (pERK2) 45 min later in the hippocampus, depending on stimulus strength. Weak IA (wIA) memory reactivation induced significant pERK2 increase compared to naïve animals, while strong IA (sIA) memory reactivation significantly decreased it. On the other hand, contextual exposure alone did not alter pERK2 levels at this time point[32]. Consistently, intrahippocampal administration of PD098059, a MEK1/2 inhibitor, 45 min after wIA retrieval, strengthened memory tested 24 h later; while the same treatment after sIA impaired long-term retention[31].

Considering that memory reconsolidation induced significant changes in extra-nuclear ERK activity, and that dimerization has been demonstrated to regulate subcellular localization of ERK activity, we wondered whether this molecular mechanism would similarly regulate memory stabilization following reactivation in mice, using the IA task. The small molecule DEL-22379 (DEL hereafter) was shown to inhibit ERK dimerization process, impairing the growth of tumor cells[13] depending on the specific driver mutation for thyroid cancer onset and progression, and with no apparent toxicity[44]. However, ERK dimerization has never been reported in nervous tissue so far. In consequence, our first experiment was aimed to characterize ERK2 dimerization in the rodent nervous system (fig. 1). To induce ERK2 dimerization, two protocols were used: 1) cLTP induced in rat primary neuronal cultures by glycine stimulation (Swanger et al., 2013) and 2) intrahippocampal stimulation with epidermal growth factor (EGF). Then, protein-enriched samples from both protocols were resolved in native polyacrylamide gels. In the first case, cultures were pre-incubated either with vehicle (VEH) or DEL, and then cLTP was induced with a previously characterized protocol[42]. As positive control, other cultures were stimulated with epidermal growth factor (EGF) which is a classical ERK1/2 pathway activator that also induces its dimerization (Casar et al., 2008). As expected, EGF stimulation protocol induced ERK2 dimerization (fig. 1A). Furthermore, cLTP also induced ERK2 dimerization and DEL pre-treatment (30 min) completely abolished it (fig. 1A).

However, primary neuronal cultures are devoid of the tissue context existing in the mouse hippocampus; so, we decided to evaluate dimerization *in vivo*. For this purpose, in the second experiment, we assessed the efficacy of DEL to inhibit ERK2 dimerization in CF-1 mice hippocampal tissue. We acutely administered either VEH or DEL solution plus either PBS (VEH) or EGF in each hemi-hippocampus of CF-1 anesthetized mice. Afterwards, mice were euthanized and we performed SDS and native western blots of protein-enriched hippocampal samples. A schematic experimental design is shown on top of figure 1B. This administration scheme was used in order to perform experimental and control treatments in the same animal. Consistent with our predictions, EGF administration altered hippocampal pERK2 levels 5 (fig. 1B left; $F_{2,13}$=5.381, p=0.0481) and 15 min later (fig. 1B right; $F_{2,13}$=8.582, p=0,01003). EGF administration induced a rapid and transient significant increase in hippocampal pERK2 at 5 min (p=0.0492) which decreased under VEH baseline levels at 15 min (p=0.01003). It is important to point out that DEL treatment did not affect EGF-induced pERK2 profile at the time points assessed (p=0.989 at 5 min; p=0.555 at 15 min in EGF-VEH vs EGF-DEL contrasts), which were also statistically different from control (p=0,036 at 5 min; p=0,0093 at 15 min in VEH-VEH vs DEL-EGF contrasts). However, ERK2 dimerization (fig. 1C) followed different kinetics. Although EGF administration did not affect dimerization at 5 min (fig. 1C left; F=0.2703; p=0.7694), dimer/monomer (dim/mon) ratio was significantly altered at 15 min (fig. 1C right; F=11.623; p=0.0044). Consistent with previous results[13], EGF alone induced a significant rise in ERK2 dimerization (p=0.014) which was prevented by DEL pre-treatment

(p=0.030) which induced dim/mon levels comparable to VEH-treated hippocampi (p=0.915). Therefore, phosphorylation and dimerization of ERK2 showed strong negative correlation 15 min after stimulation (fig. 1D, p=0.049). Thus, we can conclude that DEL prevents ERK2 dimerization induced by EGF in the treated hippocampi of CF-1 mice, without affecting its phosphorylation.

Next, we wondered whether inhibition of ERK2 dimerization has a consequence on hippocampal plasticity. In order to answer this question, we performed acute LTP experiments on hippocampal slices. Slices were pre-incubated for 30 min in the presence of VEH or DEL, a 10 min baseline fEPSP was recorded and then HFS (5 trains, 100 Hz, 10 pulses) was delivered. Neither fEPSP baseline recordings nor immediate post-HFS fEPSPs were altered by DEL treatment (fig. 1E). However, around 15 min after HFS application, DEL-treated slices begin to diverge from VEH-treated ones. In this last part of the experiment, fEPSP recordings were significantly different between treatments ($p=1.44 \times 10^{-10}$).

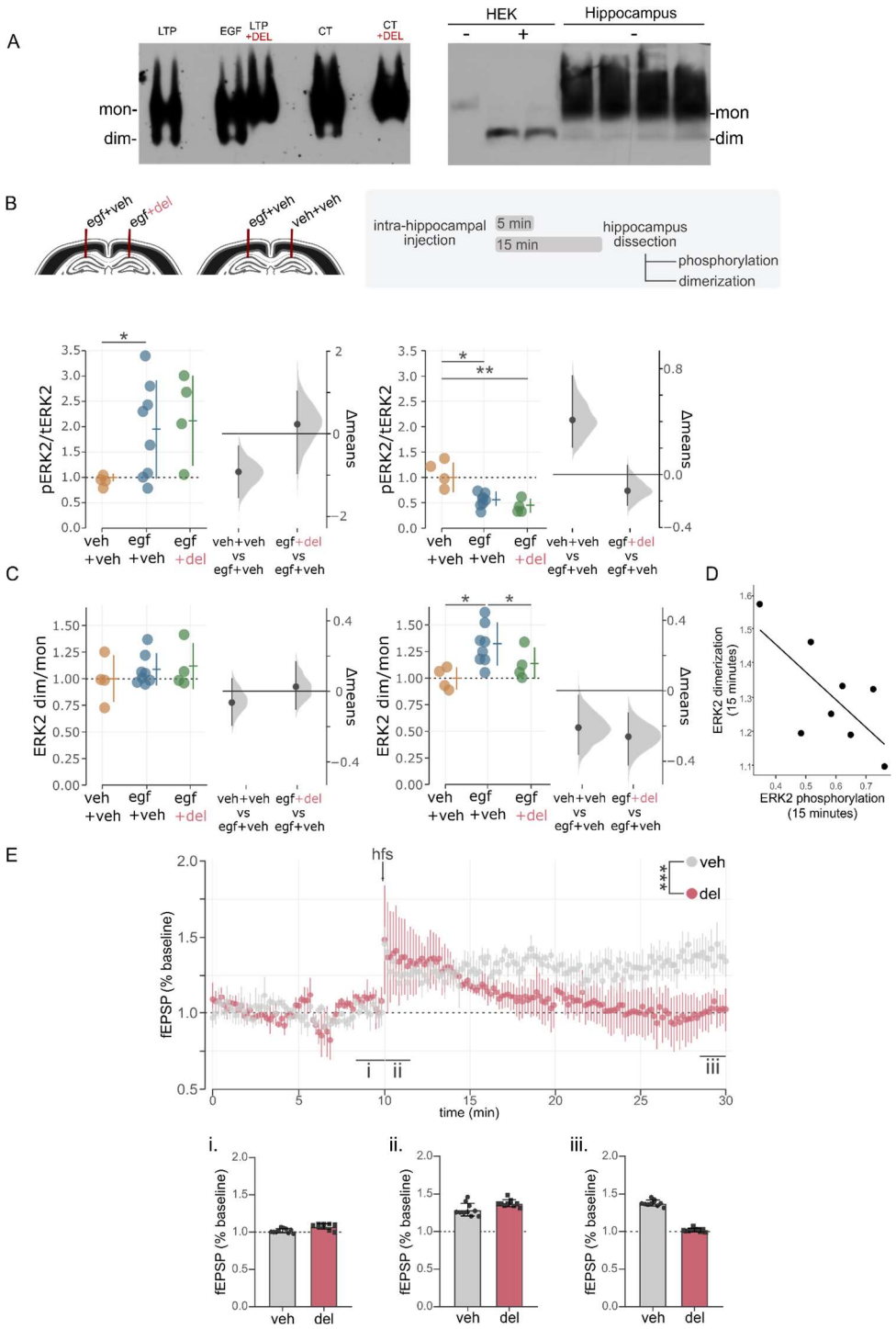

Figure 1. In vivo ERK2 dimerization in the rodent nervous system. **A)** Native PAGE western blot showing ERK2 dimers (dim) and monomers (mon) in samples from either rat neuronal primary cultures subjected to either cLTP or EGF stimulation and-or DEL treatment (left). Control and EGF-stimulated HEK-293T culture cells and CF-1 mice hippocampal protein homogenates (right). **B-C)** ERK2 phosphorylation precedes dimerization in EGF-stimulated CF-1 mice hippocampal tissue. Schematic experimental design is shown on **top** of fig. B). Hippocampal ERK2 phosphorylation **(B)** and dimerization **(C)** were assessed 5 (left) or 15 (right) min after *in vivo* local EGF plus VEH or DEL administration. Dimer / monomer (dim/mon) ratios were normalized against "veh+veh" mean value in each case. Circles represent individual mice measurements, single lines represent mean ± s.d., and estimation plots shown on the right of each graph represent the difference between means (black dot) and the bootstrapped distribution of means (grey area) with 95% confidence intervals. *****, $p < 0.05$; ******, $p < 0.01$ in Tukey comparisons. n = 4 mice / group. **D)** Pearson correlation between ERK2 phosphorylation and dimerization assessed at 15 min in figures B and C. $R^2 = 0.71$; $p < 0.05$. **E)** Inhibition of ERK2 dimerization impairs LTP in CA1 hippocampal acute

slices. Circles represent the mean of 4 replicates and single lines represent s.d. Three points of interest are indicated throughout the recording: immediately before stimulation (i), immediately after stimulation (ii), and approx. 18-20 min after stimulation (iii). Bars in i), ii) and iii) are the mean ± s.d. of 100 sec recordings. ***, $p < 0.05$ (repeated measures comparison between VEH- and DEL-treated groups). n = 4 mice / group.

Memory reactivation after Weak IA decreases hippocampal ERK dimerization

Considering that ERK dimerization can modulate hippocampal plasticity, and that IA memory reconsolidation is fine-tuned by extra-nuclear ERK signaling at 45 min (Krawczyk et al., 2015), we wondered whether its dimerization is regulated by memory reactivation in the hippocampus at this time point. Therefore, we trained animals in either strong or weak versions of the IA task and subjected them to memory reactivation (RE) 48 h later. As a control, identically trained animals were not exposed to reactivation (NR). We euthanised all four groups of animals 45 min after reactivation or the corresponding time for NR groups and dissected their hippocampi in order to perform native western blot assays and ERK dimerization assessment.

Reexposure to the IA context 48 h after strong TR did not induce evident changes in ERK2 dimerization levels related to NR control animals 45 min later (fig. 2; t_{13}=0.161; p=0.873). Meanwhile, weak IA memory reactivation showed significant decrease in ERK2 dimerization relative to the NR control group (t_{14}=2.569; p=0.0223). The observation that memory reactivation induced differential ERK2 dimerization depending on TR strength suggested the possibility that this molecular mechanism plays a role in memory reconsolidation as well.

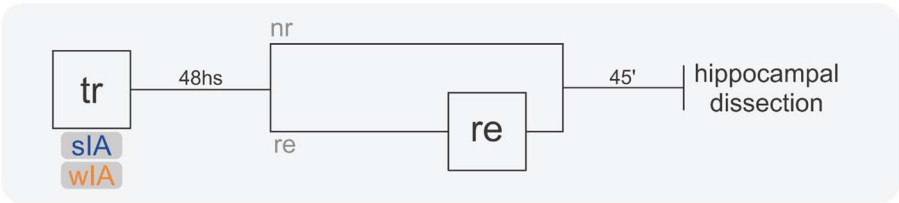

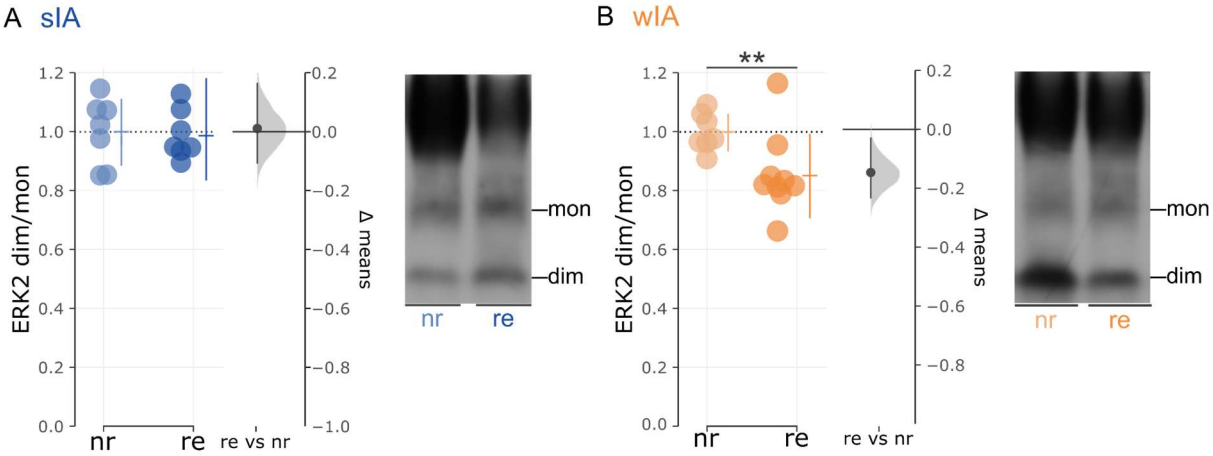

Figure 2. Hippocampal ERK2 dimerization after memory reactivation. **Top)** Schematic experimental design for hippocampal ER2 dimerization assessment. **Bottom)** Hippocampal ERK2 dimerization assessment by native

PAGE western blots 45 after either sIA **(A**, yellow dataset**)** or wIA **(B**, blue dataset**)** memory reactivation. Dim/ mon ratios are normalized against nr mean value for each experiment. Color circles indicate individual values and error bars shown on the right of each set depict mean ± s.d. values. Estimation plots shown on the right of each graph represent the difference between means (black dot) and the bootstrapped distribution of means (grey area) with 95% confidence intervals. Representative western blots are also shown (right). *****, $p < 0.05$; ******, $p < 0.01$ in Tukey comparisons. n = 7-9 / group.

Post-retrieval hippocampal ERK2 dimerization supports strong IA memories

Given that ERK2 dimerization may be involved in memory reconsolidation, memory reactivation, which triggers labilization, should be affected by its inhibition. In consequence, we first evaluated whether ERK2 dimerization was affected by intrahippocampal DEL administration after memory reactivation. For this experiment, all animals were injected either VEH or DEL in both hippocampi 35 min after RE or the corresponding time for NR animals (fig. 3A, upper scheme) and 10 min later animals were euthanized and their hippocampi were removed and homogenized. As shown in figure 3A (lower panel), reactivation did not induce changes in ERK2 dimerization levels ($F_{2,21}$=5.559; p=0.0115; p=0.336 in NR-VEH vs RE-VEH contrast). However, hippocampal DEL injection after reactivation induced a striking tendency to decrease hippocampal ERK2 dimerization levels of almost 20% compared to RE-VEH group (p=0.0567) and a significant decrease related to NR-VEH animals (p=0.0102).

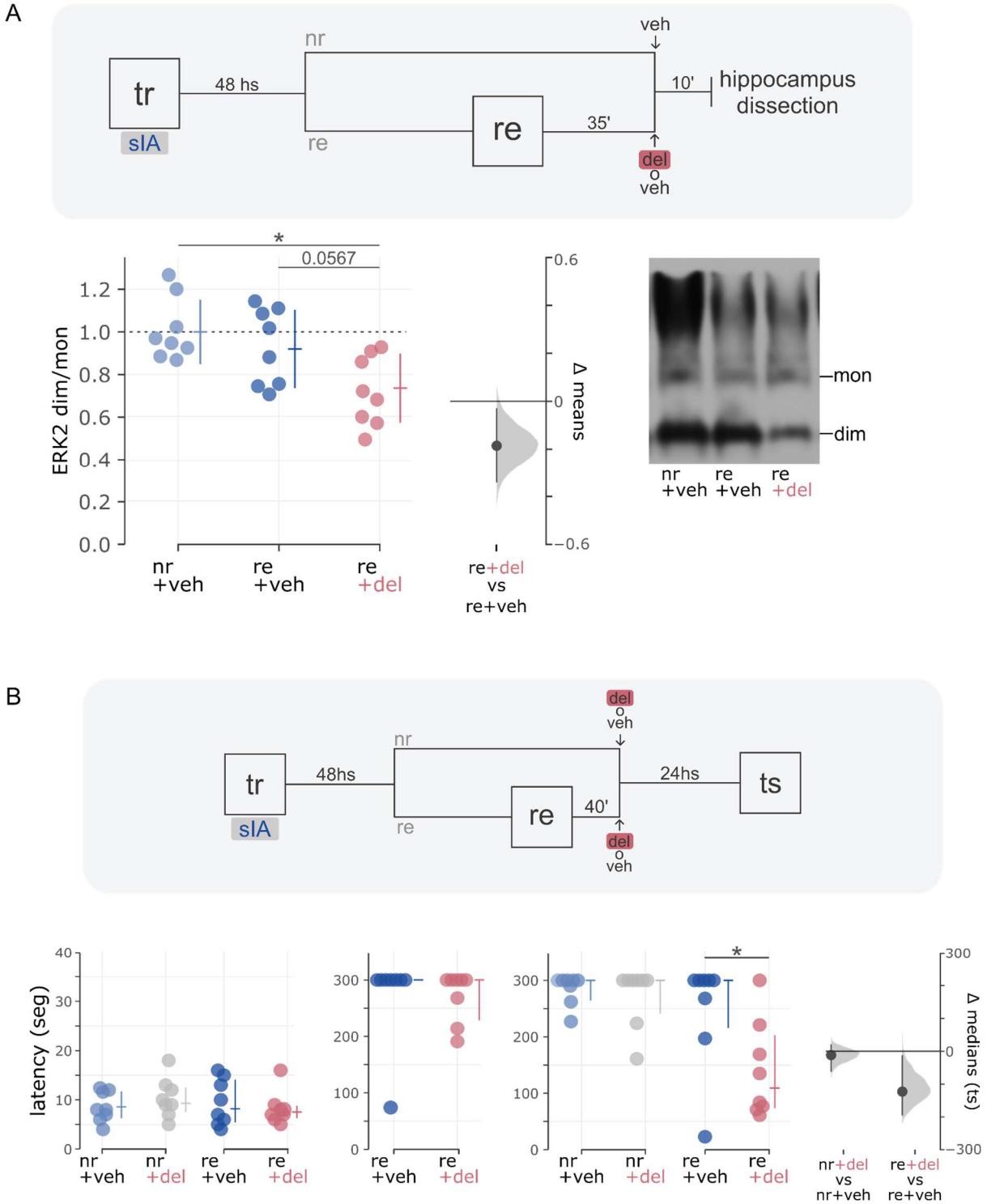

Figure 3. Role of hippocampal ERK2 dimerization after strong IA memory reactivation. **A)** DEL decreases hippocampal ERK2 dimerization after strong IA memory reactivation. Schematic experimental design for hippocampal ERK2 dimerization assessment is shown **(top)**. Hippocampal ERK2 dimerization was assessed 45 min after strong IA memory reactivation and 10 min after VEH or DEL intra-hippocampal administration. Dimer to monomer ratios were normalized against nr mean value for each experiment. Color circles indicate individual values and error bars shown on the right of each dataset depict mean ± s.d. values. Estimation plots shown on the right of each graph represent the difference between means (black dot) and the bootstrapped distribution of means (grey area) with 95% confidence intervals. Representative western blots are also shown (right). *, $p < 0.05$; **, $p < 0.01$ in Tukey adjusted *post hoc* comparisons. n = 8 / group. **B)** Inhibition of hippocampal ERK2 dimerization after strong

IA memory reactivation impairs LTM. Schematic experimental design is shown **(top)**. Color circles indicate individual latencies to step through values and error bars shown on the right of each set depict median ± IQ intervals (tr) or mean ± s.d. values (re and ts). Estimation plots shown on the right of ts graph represent the difference between means (black dot) and the bootstrapped distribution of means (grey area) with 95% confidence intervals. *****, $p < 0.05$; ******, $p < 0.01$ in Tukey adjusted *post hoc* comparisons. n = 8 / group.

Next, we asked whether specific ERK2 dimerization levels are necessary for strong IA memory re-stabilization. We aimed to answer this question by administering VEH or DEL 40 min after strong IA memory reactivation and tested retention 24 h later (fig. 3B, upper panel). All groups performed similarly during training and reactivated groups expressed strong retention during reexposure to the training context (fig. 3B, lower panel). However, there was a significant interaction between reactivation and drug treatment on latencies during the test session ($F_{2,28}$=5.291; p=0.029), with statistically significant main effect of reactivation protocol ($F_{1,28}$=9.714; p=0.0041) and a tendency in drug treatment main effect ($F_{1,28}$=4.102; p=0.0524). Thus, while latencies from VEH- and DEL-injected NR animals did not differ statistically (p=0.9833), DEL treatment after memory reactivation induced a significant decrease in latencies compared to the VEH group (p=0,0287). General response levels during TS were similar, as latencies from VEH-injected groups were not statistically different (p=0.6847). Furthermore, this impairment lasted for at least a week (suppl. fig. 1; p=0.013). This long-lasting impairment suggests a specific effect on the reconsolidation process. In consequence, basal ERK2 dimerization levels seem to be required for strong IA memory reconsolidation.

Inhibiting hippocampal ERK dimerization after reactivation strengthens weak IA memories

We showed that weak IA memory reactivation induced a decrease in ERK2 dim/mon ratio in mice hippocampi (fig. 2B). Consequently, we wondered whether intra-hippocampal DEL administration after weak IA reactivation would have any consequence on LTM retention. We trained 4 groups of animals in a weak IA task and submitted two of them to memory reactivation (RE, non-reactivated groups: NR), 48 h later. Performance during training was similar in all groups. As expected, RE groups expressed median latencies of ≈150 sec during the reactivation session. One NR and one RE groups of animals were administered VEH and the other two groups were injected DEL intrahippocampal 40 min after the reactivation time. All groups were tested 24 h later (fig. 4A). Latencies to step through during the test session exhibited a significant interaction between reactivation procedure and drug treatment ($F_{2,30}$=13.254; p=0.0010). In this case, a statistically significant main effect of drug treatment ($F_{1,30}$=5.459; p=0.0263) and no effect of reactivation protocol ($F_{1,30}$=3.935; p=0.0564) was disclosed. Surprisingly, in RE-animals, the DEL-injected group showed significantly higher latencies than the VEH-injected one (p=0.0049), and this effect was specific for the reactivated groups as NR animals did not show significant differences in latencies between VEH and DEL treatment during test (p=0.3786). Moreover, both VEH-treated groups expressed similar latencies during the test session (p=0.2730). Not only did intrahippocampal DEL administration after a weak IA memory reactivation improve retention, but it also seemed to have drastically increased the proportion of animals exhibiting higher latencies during TS compared to RE (suppl. fig.2, right panel). Notably, a significant positive correlation was observed between RE and TS response levels in DEL-RE animals (suppl. fig. 2; R^2=0.73; p=0.025), which differed from the VEH-RE group (suppl. fig. 2; R^2=0.42; p=0.27).

A

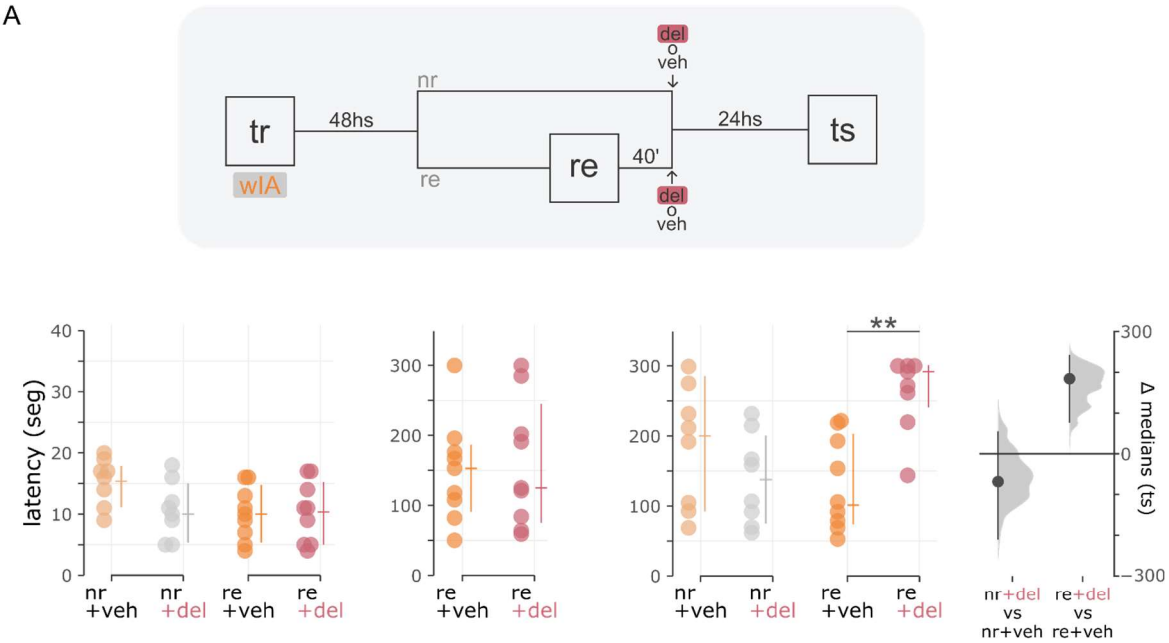

B

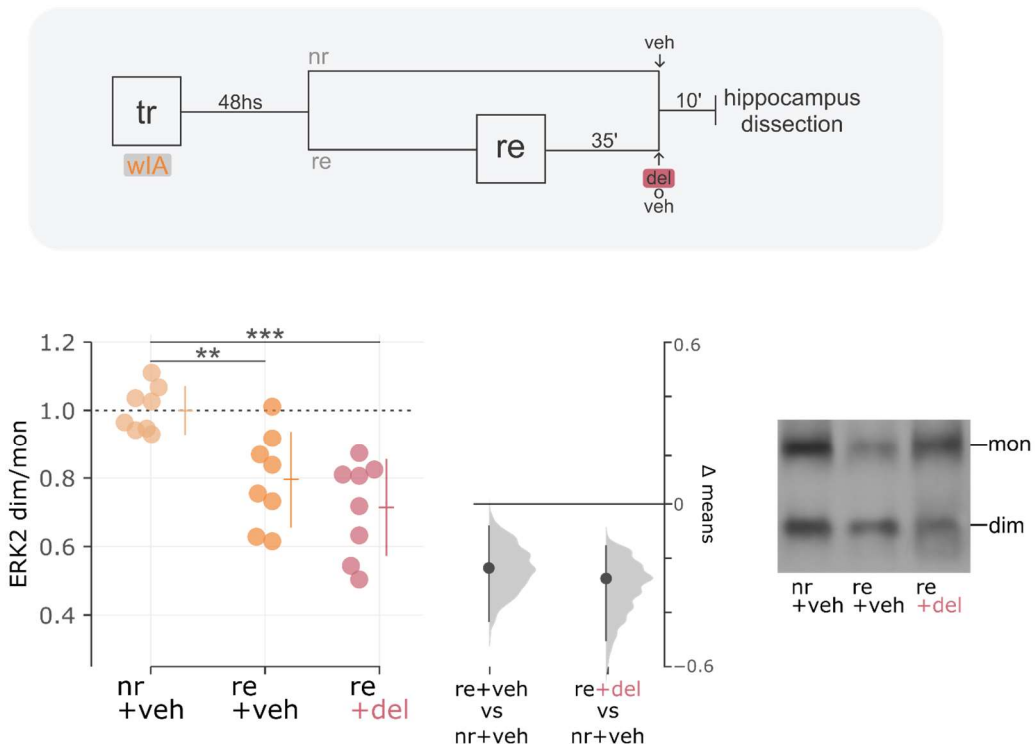

Figure 4. Role of hippocampal ERK2 dimerization after weak IA memory reactivation. **A)** Inhibition of hippocampal ERK2 dimerization after strong IA memory reactivation improves LTM. Schematic experimental design is shown on top. Color circles indicate individual latencies to step through values during tr (left), re (center) and ts (right). Error bars shown on the right of each dataset depict median ± IQ intervals. Estimation plots shown on the right of ts graph represent the difference between means (black dot) and the bootstrapped distribution of means (grey area) with 95% confidence intervals. *, $p < 0.05$; **, $p < 0.01$ in Tukey adjusted *post hoc* comparisons. n = 8 - 9 / group. **B)** Hippocampal ERK2 dimerization decreases after weak IA memory reactivation. Schematic experimental design is shown on top. Color circles indicate individual values and error bars shown on the right of each dataset depict mean ± s.d. values. Estimation plots shown on the right of each graph represent the difference between means (black dot) and the bootstrapped distribution of means (grey area) with 95% confidence intervals.

Representative western blots are also shown (right). *, $p < 0.05$; **, $p < 0.01$ in Tukey adjusted *post hoc* comparisons. n = 8 / group.

Finally, ERK2 dimerization levels were significantly affected by reactivation also in VEH/DEL-injected animals as well ($F_{2,21}$=13.254; p=0.0002). In contrast to what we observed after sIA training, wIA memory reactivation led to a significant decrease in ERK2 dimerization (see fig. 2B) which was also observed after VEH-administration in mice hippocampi (fig. 4B; p=0.0064). However, DEL- injection did not affect ERK2 dimerization levels following memory reactivation (p=0.3753), though these levels were significantly different from those in the control group NR-VEH (p=0.0003).

Discussion

In this work, we show for the first time that ERK2 dimerization constitutes a regulatory key step from ERK signaling involved in plasticity, learning and memory processes. Several lines of evidence indicate that subcellular localization of a particular intracellular signaling pathway is crucial for a specific biological outcome[12,45,46]. In the central nervous system for example, it was shown that NF-kappaB might be regulating different phenomena related to neural plasticity, memory and learning processes depending on its subcellular localization[47,48]. Over the past decade, oncological research has paved the way for the development of drugs targeting key pathways to reverse pathological conditions. Most of these pathways have also been linked to learning and memory processes. However, their regulatory mechanisms often remain unveiled within the context of the nervous system. ERK signaling is an example. It is well known that ERK phosphorylation is needed for neural plasticity and cognitive processes and its deregulation often results in pathological conditions. Nevertheless, the Crespo-Baraja lab postulated that ERK dimerization regulates subcellular location of its activity, thereby influencing phosphorylation of specific targets and ultimately the cellular fate[12,13]. However, no other reports have investigated dimerization function in the nervous system, despite extensive studies on ERK activation in these tissues[reviewed in 9].

As a first step, we demonstrated that ERK dimerization occurred in neural tissue both, *in vitro*, in primary neuronal cultures; and *in vivo*, in the hippocampus of CF-1 mice. Primary neuronal cultures stimulated with either EGF or a glycine-based cLTP protocol showed ERK2 dimerization which was inhibited by DEL pre-treatment (fig. 1A). Moreover, upon EGF stimulation, DEL treatment inhibited *in vivo* hippocampal ERK2 dimerization without affecting its phosphorylation (fig. 1B and 1C). Previous research has shown that EGF stimulation induces ERK dimerization in cancer cells[13]. In physiological contexts, the concentration of EGF plays a critical role in determining cellular responses, with variations in EGF dosage influencing the transition between migratory and proliferative states[49]. Thus, low EGF concentration, typical of paracrine signaling in early stages of wound closure, is inadequate to trigger robust proliferative ERK signals in the cytoplasm. However, it led to pro-migratory signaling that induced an increase in cell migration dependent on KSR-ERK activation at the plasma membrane[49]. The EGF concentration used in our culture experiments were consistent with those used in Herrero and colleagues[13] for HEK293T cells and with those promoting proliferation in MCF7 cells[49]. Here, we were able to reproduce those experiments and that served as a control to evaluate ERK2 dimerization in rodents' nervous tissue (fig. 1A). Regardless of the stimulation duration, EGF has been demonstrated to induce rapid and

transient ERK phosphorylation in PC12 cells, which promotes cell proliferation[50]. We observed similar kinetics in our study. As many other tissues, brain cells express EGFR and its activation regulates neurite outgrowth as well as other outputs related to neuronal homeostasis[51]. However, it is well known that different ligands are capable of inducing different ERK activation kinetics and cellular outputs[52]. It remains to be determined how ERK dimerization is altered according to ligand specificity and its biological consequences, specifically in neurons.

ERK dimers in plasticity

We have recently discussed the role of ERK signaling in plasticity[9]. Hippocampal plasticity has been proposed as a cellular correlate of experience-coding leading to memory formation and storage. In consequence, a plausible hypothesis suggests that ERK dimerization might regulate memory processes. Since the initial work by English and Sweatt[3] showing that ERK inhibition blocked HFS-induced LTP in rat hippocampal area CA1, several authors have provided evidence in favor of its participation in these processes[5,17,53,54] and as we mentioned before, different stimuli acting on the same intracellular signaling pathway might cause alternative cellular fates depending on the set of scaffolding proteins engaged[12]. As a general hallmark, it has been shown that HFS protocol applied in the Schaffer Collaterals inputs to CA1 area induced ERK2 phosphorylation in rodents, and blocking ERK phosphorylation previous to LTP induction prevented longer lasting forms of LTP[reviewed in 9]. In our study, we demonstrated that inhibiting ERK dimerization with DEL treatment on acute slices also impaired hippocampal LTP shortly after electrical stimulation. These findings suggest that both ERK phosphorylation and dimerization are crucial for the establishment of LTP. Additionally, since ERK dimerization and phosphorylation target different neuronal compartments, it is possible that at least two distinct pathways are triggered during ERK activation. Moreover, memory processes have been shown to involve activation of multiple receptor systems which may lead to activation of other molecular pathways affecting ERK signaling and consequently, determining different kinetics and activated targets. In consequence, it can be expected that ERK2 dimerization might be also involved in LTP induction.

ERK in IA LTM reconsolidation

To this day, ERK signaling was classically considered as a determining pathway for LTM consolidation. It was also proposed as one of the molecules related to memory labilization and reconsolidation. It is worth noting that ERK's role in plasticity and memory processes has been attributed almost exclusively to phosphorylation, leaving the possibility of other post-translational modifications regulating these processes largely unexplored. Our results show that hippocampal inhibition of ERK dimerization impairs sIA memory reconsolidation. However, the same manipulation of the pathway induced memory enhancement when a weak IA task was used, suggesting that the same brain structure might engage opposing processes depending on the strength of the consolidated memory. These results are consistent with the idea that the restabilization process that takes place after either sIA or wIA memory retrieval would be extremely specific and might engage distinct neural circuits (Milekic 2007). Alternatively, different stimuli (e.g. ligand identity and/or concentration) may activate distinct components from ERK pathways which could in turn be transduced in spatially distinct ERK pools that regulate various cellular outputs. For instance, a strong stimulus could trigger protein translation via ERK activation and promote gene transcription via ERK nuclear translocation. In this scenario, ERK inhibition would impair memory by disrupting these

processes. Conversely, after a weak stimulus, ERK inhibition might enhance memory by promoting protein synthesis through alternative pathways. This could compensate for reduced ERK activation and facilitate memory reconsolidation. Supporting this hypothesis, it was observed that protein synthesis inhibition after reactivation exerted differential effects on memory restabilization of an IA task in mice according to the area infused. Thus, protein synthesis was required in the amygdala in order to support memory reconsolidation while in the hippocampus and mPFC it was necessary to enhance retention[55]. More experiments could be performed in order to support this theory.

Our experiments also confirmed that the effect of hippocampal ERK dimerization is specific to the reconsolidation process by showing that NR animals´ latencies to step through were not affected by intra-hippocampal DEL injection (figures 3B and 4A). Regarding sIA memory impairment following DEL administration, we observed persistent impairment after one week (suppl. fig. 1), ruling out spontaneous recovery of the original memory which would have suggested the possibility of an extinction process.

In the present manuscript, we showed for the first time evidence of ERK2 dimerization playing a critical role in the central nervous system. Our findings reveal that ERK2 dimerization is essential for hippocampal plasticity and memory reconsolidation, introducing a novel mechanism of ERK2 regulation in the brain. Future studies will likely elucidate the other molecular players recruited by this new mechanism.

Funding

This work was supported by the following grants: Agencia Nacional de Promoción de la Investigación, el Desarrollo Tecnológico y la Innovación (ANPCYT PICT2016 0295, ANPCYT PICT2020 01534 and PICT2015 1199), Consejo Nacional de Investigaciones Científicas y Técnicas (CONICET PIP 2014-2016 No. 11220130100519CO) and University of Buenos Aires (UBACYT 2018-2021 - 20020170100390BA and 2014-2017 - 20020130200283BA), Argentina.

References

1. Bliss, T. V. P. & Lømo, T. Long-lasting potentiation of synaptic transmission in the dentate area of the anaesthetized rabbit following stimulation of the perforant path. *J. Physiol.* **232**, 331–356 (1973).
2. Bliss, T. V. & Collingridge, G. L. A synaptic model of memory: long-term potentiation in the hippocampus. *Nature* **361**, 31–39 (1993).
3. English, J. D. & Sweatt, J. D. Activation of p42 mitogen-activated protein kinase in hippocampal long term potentiation. *J. Biol. Chem.* **271**, 24329–24332 (1996).
4. Martin, K. C. *et al.* MAP kinase translocates into the nucleus of the presynaptic cell and is required for long-term facilitation in Aplysia. *Neuron* **18**, 899–912 (1997).
5. Atkins, C. M., Selcher, J. C., Petraitis, J. J., Trzaskos, J. M. & Sweatt, J. D. The MAPK cascade is required for mammalian associative learning. *Nat. Neurosci.* **1**, 602–609 (1998).

6. Blum, S., Moore, A. N., Adams, F. & Dash, P. K. A mitogen-activated protein kinase cascade in the CA1/CA2 subfield of the dorsal hippocampus is essential for long-term spatial memory. *J. Neurosci. Off. J. Soc. Neurosci.* **19**, 3535–3544 (1999).
7. Walz, R. *et al.* Effects of post-training infusions of a mitogen-activated protein kinase kinase inhibitor into the hippocampus or entorhinal cortex on short- and long-term retention of inhibitory avoidance. *Behav. Pharmacol.* **10**, 723–730 (1999).
8. Schafe, G. E. *et al.* Activation of ERK/MAP kinase in the amygdala is required for memory consolidation of pavlovian fear conditioning. *J. Neurosci. Off. J. Soc. Neurosci.* **20**, 8177–8187 (2000).
9. Ojea Ramos, S., Feld, M. & Fustiñana, M. S. Contributions of extracellular-signal regulated kinase 1/2 activity to the memory trace. *Front. Mol. Neurosci.* **15**, (2022).
10. Lavoie, H., Gagnon, J. & Therrien, M. ERK signalling: a master regulator of cell behaviour, life and fate. *Nat. Rev. Mol. Cell Biol.* **21**, 607–632 (2020).
11. Casar, B., Pinto, A. & Crespo, P. Essential role of ERK dimers in the activation of cytoplasmic but not nuclear substrates by ERK-scaffold complexes. *Mol. Cell* **31**, 708–721 (2008).
12. Casar, B. & Crespo, P. ERK Signals: Scaffolding Scaffolds? *Front. Cell Dev. Biol.* **4**, (2016).
13. Herrero, A. *et al.* Small Molecule Inhibition of ERK Dimerization Prevents Tumorigenesis by RAS-ERK Pathway Oncogenes. *Cancer Cell* **28**, 170–182 (2015).
14. Ahn, N. G. PORE-ing over ERK substrates. *Nat. Struct. Mol. Biol.* **16**, 1004–1005 (2009).
15. Earnest, S., Khokhlatchev, A., Albanesi, J. P. & Barylko, B. Phosphorylation of dynamin by ERK2 inhibits the dynamin-microtubule interaction. *FEBS Lett.* **396**, 62–66 (1996).
16. Gong, R. & Tang, S.-J. Mitogen-activated protein kinase signaling is essential for activity-dependent dendritic protein synthesis. *Neuroreport* **17**, 1575–1578 (2006).
17. Kelleher, R. J., 3rd, Govindarajan, A., Jung, H.-Y., Kang, H. & Tonegawa, S. Translational control by MAPK signaling in long-term synaptic plasticity and memory. *Cell* **116**, 467–479 (2004).
18. Kneussel, M. & Wagner, W. Myosin motors at neuronal synapses: drivers of membrane transport and actin dynamics. *Nat. Rev. Neurosci.* **14**, 233–247 (2013).
19. Schrader, L. A. *et al.* ERK/MAPK regulates the Kv4.2 potassium channel by direct phosphorylation of the pore-forming subunit. *Am. J. Physiol. Cell Physiol.* **290**, C852-861 (2006).
20. Boggio, E. M., Putignano, E., Sassoè-Pognetto, M., Pizzorusso, T. & Giustetto, M. Visual stimulation activates ERK in synaptic and somatic compartments of rat cortical neurons with parallel kinetics. *PloS One* **2**, e604 (2007).
21. Pirbhoy, P. S., Farris, S. & Steward, O. Synaptically driven phosphorylation of ribosomal protein S6 is differentially regulated at active synapses versus dendrites and cell bodies by MAPK and PI3K/mTOR signaling pathways. *Learn. Mem. Cold Spring Harb. N* **24**, 341–357 (2017).
22. Fukuda, M., Gotoh, I., Adachi, M., Gotoh, Y. & Nishida, E. A novel regulatory mechanism in the mitogen-activated protein (MAP) kinase cascade. Role of nuclear export signal of MAP kinase kinase. *J. Biol. Chem.* **272**, 32642–32648 (1997).
23. Brunet, A. *et al.* Nuclear translocation of p42/p44 mitogen-activated protein kinase is required for growth factor-induced gene expression and cell cycle entry. *EMBO J.* **18**, 664–674 (1999).
24. Vetterkind, S., Poythress, R. H., Lin, Q. Q. & Morgan, K. G. Hierarchical scaffolding of an ERK1/2 activation pathway. *Cell Commun. Signal. CCS* **11**, 65 (2013).
25. Gao, C. *et al.* IQGAP1 regulates NR2A signaling, spine density, and cognitive processes. *J. Neurosci. Off. J. Soc. Neurosci.* **31**, 8533–8542 (2011).
26. Albert-Gascó, H., Ros-Bernal, F., Castillo-Gómez, E. & Olucha-Bordonau, F. E. MAP/ERK Signaling in Developing Cognitive and Emotional Function and Its Effect on Pathological and Neurodegenerative Processes. *Int. J. Mol. Sci.* **21**, 4471 (2020).
27. Nader, K., Schafe, G. E. & Le Doux, J. E. Fear memories require protein synthesis in the amygdala for reconsolidation after retrieval. *Nature* **406**, 722–726 (2000).
28. Sara, S. J. Retrieval and reconsolidation: toward a neurobiology of remembering. *Learn. Mem. Cold Spring Harb. N* **7**, 73–84 (2000).

29. Dudai, Y. & Eisenberg, M. Rites of passage of the engram: reconsolidation and the lingering consolidation hypothesis. *Neuron* **44**, 93–100 (2004).
30. Feld, M., Dimant, B., Delorenzi, A., Coso, O. & Romano, A. Phosphorylation of extra-nuclear ERK/MAPK is required for long-term memory consolidation in the crab Chasmagnathus. *Behav. Brain Res.* **158**, 251–261 (2005).
31. Krawczyk, M. C. *et al.* Memory reconsolidation of an inhibitory avoidance task in mice involves cytosolic ERK2 bidirectional modulation. *Neuroscience* **294**, 227–237 (2015).
32. Krawczyk, M. C. *et al.* Reconsolidation-induced memory persistence: Participation of late phase hippocampal ERK activation. *Neurobiol. Learn. Mem.* **133**, 79–88 (2016).
33. Krawczyk, M. C., Millan, J., Blake, M. G., Feld, M. & Boccia, M. M. Relevance of ERK1/2 Post-retrieval Participation on Memory Processes: Insights in Their Particular Role on Reconsolidation and Persistence of Memories. *Front. Mol. Neurosci.* **12**, 95 (2019).
34. Feld, M. *et al.* Decrease of ERK/MAPK overactivation in prefrontal cortex reverses early memory deficit in a mouse model of Alzheimer's disease. *J. Alzheimers Dis. JAD* **40**, 69–82 (2014).
35. Rivero-Echeto, M. C. *et al.* Simultaneous administration of cocaine and caffeine dysregulates HCN and T-type channels. *Psychopharmacology (Berl.)* **238**, 787–810 (2021).
36. *Paxinos and Franklin's the Mouse Brain in Stereotaxic Coordinates*. (2019).
37. Boccia, M. M., Acosta, G. B., Blake, M. G. & Baratti, C. M. Memory consolidation and reconsolidation of an inhibitory avoidance response in mice: effects of i.c.v. injections of hemicholinium-3. *Neuroscience* **124**, 735–741 (2004).
38. Blake, M. G., Boccia, M. M. & Baratti, C. M. Behavioral differences on memory retrieval between two variants of step-through inhibitory avoidance task in mice. *Neurosci. Lett.* **444**, 102–105 (2008).
39. Blake, M. G., Krawczyk, M. C., Baratti, C. M. & Boccia, M. M. Neuropharmacology of memory consolidation and reconsolidation: Insights on central cholinergic mechanisms. *J. Physiol. Paris* (2014) doi:10.1016/j.jphysparis.2014.04.005.
40. Acutain, M. F. *et al.* Reduced Expression of Hippocampal GluN2A-NMDAR Increases Seizure Susceptibility and Causes Deficits in Contextual Memory. *Front. Neurosci.* **15**, 644100 (2021).
41. Kaech, S. & Banker, G. Culturing hippocampal neurons. *Nat. Protoc.* **1**, 2406–2415 (2006).
42. Swanger, S. A., He, Y. A., Richter, J. D. & Bassell, G. J. Dendritic GluN2A Synthesis Mediates Activity-Induced NMDA Receptor Insertion. *J. Neurosci.* **33**, 8898–8908 (2013).
43. Pinto, A. & Crespo, P. Analysis of ERKs' dimerization by electrophoresis. *Methods Mol. Biol. Clifton NJ* **661**, 335–342 (2010).
44. Zaballos, M. A. *et al.* Inhibiting ERK dimerization ameliorates BRAF-driven anaplastic thyroid cancer. *Cell. Mol. Life Sci. CMLS* **79**, 504 (2022).
45. Afinanisa, Q., Cho, M. K. & Seong, H.-A. AMPK Localization: A Key to Differential Energy Regulation. *Int. J. Mol. Sci.* **22**, 10921 (2021).
46. Formoso, K., Lezoualc'h, F. & Mialet-Perez, J. Role of EPAC1 Signalosomes in Cell Fate: Friends or Foes? *Cells* **9**, 1954 (2020).
47. Salles, A., Romano, A. & Freudenthal, R. Synaptic NF-kappa B pathway in neuronal plasticity and memory. *J. Physiol. Paris* **108**, 256–262 (2014).
48. Salles, A. *et al.* Hippocampal dynamics of synaptic NF-kappa B during inhibitory avoidance long-term memory consolidation in mice. *Neuroscience* **291**, 70–80 (2015).
49. Brüggemann, Y., Karajannis, L. S., Stanoev, A., Stallaert, W. & Bastiaens, P. I. H. Growth factor-dependent ErbB vesicular dynamics couple receptor signaling to spatially and functionally distinct Erk pools. *Sci. Signal.* **14**, eabd9943 (2021).
50. Traverse, S., Gomez, N., Paterson, H., Marshall, C. & Cohen, P. Sustained activation of the mitogen-activated protein (MAP) kinase cascade may be required for differentiation of PC12 cells. Comparison of the effects of nerve growth factor and epidermal growth factor. *Biochem. J.* **288**, 351–355 (1992).
51. Romano, R. & Bucci, C. Role of EGFR in the Nervous System. *Cells* **9**, 1887 (2020).

52. Miningou, N. & Blackwell, K. T. The road to ERK activation: Do neurons take alternate routes? *Cell. Signal.* **68**, 109541 (2020).
53. Impey, S. *et al.* Cross talk between ERK and PKA is required for Ca2+ stimulation of CREB-dependent transcription and ERK nuclear translocation. *Neuron* **21**, 869–883 (1998).
54. Selcher, J. C. *et al.* A Role for ERK MAP Kinase in Physiologic Temporal Integration in Hippocampal Area CA1. *Learn. Mem.* **10**, 26–39 (2003).
55. Fukushima, H. *et al.* Enhancement of fear memory by retrieval through reconsolidation. *eLife* **3**, e02736 (2014).